



This is a repository copy of *Genome-wide association studies of autoimmune vitiligo identify 23 new risk loci and highlight key pathways and regulatory variants*.

White Rose Research Online URL for this paper:
<http://eprints.whiterose.ac.uk/103362/>

Version: Accepted Version

Article:

Jin, Y., Andersen, G., Yorgov, D. et al. (41 more authors) (2016) Genome-wide association studies of autoimmune vitiligo identify 23 new risk loci and highlight key pathways and regulatory variants. *Nature Genetics*, 48. pp. 1418-1424. ISSN 1061-4036

<https://doi.org/10.1038/ng.3680>

Reuse

Unless indicated otherwise, fulltext items are protected by copyright with all rights reserved. The copyright exception in section 29 of the Copyright, Designs and Patents Act 1988 allows the making of a single copy solely for the purpose of non-commercial research or private study within the limits of fair dealing. The publisher or other rights-holder may allow further reproduction and re-use of this version - refer to the White Rose Research Online record for this item. Where records identify the publisher as the copyright holder, users can verify any specific terms of use on the publisher's website.

Takedown

If you consider content in White Rose Research Online to be in breach of UK law, please notify us by emailing eprints@whiterose.ac.uk including the URL of the record and the reason for the withdrawal request.



eprints@whiterose.ac.uk
<https://eprints.whiterose.ac.uk/>

Enhanced genome-wide association studies of autoimmune vitiligo identify 23 novel loci and highlight key pathobiological pathways and causal regulatory variation

Ying Jin^{1,2}, Genevieve Andersen¹, Daniel Yorgov³, Tracey M Ferrara¹, Songtao Ben¹, Kelly M Brownson¹, Paulene J Holland¹, Stanca A Birlea^{1,4}, Janet Siebert⁵, Anke Hartmann⁶, Anne Lienert⁶, Rosalie M Luiten⁷, Albert Wolkerstorfer⁷, JP Wietze van der Veen^{7,8}, Nanja van Geel, Jo Lambert⁹, Dorothy C Bennett¹⁰, Alain Taïeb¹¹, Khaled Ezzedine¹¹, E Helen Kemp¹², David J Gawkrödger¹³, Anthony P Weetman¹², Sulev Koks¹⁴, Ele Prans¹⁴, Külli Kingo¹⁵, Maire Karelson¹⁵, Margaret R Wallace¹⁶, Wayne T McCormack¹⁷, Andreas Overbeck¹⁸, Silvia Moretti¹⁹, Roberta Colucci¹⁹, Mauro Picardo²⁰, Nanette B Silverberg^{21,22}, Mats Olssen²³, Yan Valle²⁴, Igor Korobko^{24,25}, Markus Böhm²⁶, Henry Lim²⁷, Iltefat Hamzavi²⁷, Li Zhou²⁷, Qing-Sheng Mi²⁷, Pamela R. Fain^{1,2}, Stephanie A Santorico^{1,3}, & Richard A Spritz^{1,2}

¹Human Medical Genetics and Genomics Program and ²Department of Pediatrics, University of Colorado School of Medicine, Aurora, Colorado, USA. ³Department of Mathematical and Statistical Sciences, University of Colorado Denver, Denver, Colorado, USA. ⁴Department of Dermatology, University of Colorado School of Medicine, Aurora, Colorado, USA.

⁵CytoAnalytics, Denver, Colorado, USA. ⁶Department of Dermatology, University Hospital Erlangen, Erlangen, Germany. ⁷Netherlands Institute for Pigment Disorders, Department of Dermatology, Academic Medical Centre University of Amsterdam, Amsterdam, The Netherlands. ⁸Department of Dermatology, Medical Centre Haaglanden, The Hague, The Netherlands. Department of Dermatology, Ghent University Hospital, Ghent, Belgium.

¹⁰Division of Biomedical Sciences, St. George's, University of London, London, UK. ¹¹Centre de Référence des maladies rares de la peau, Department of Dermatology, Hôpital St.-André, Bordeaux, France. ¹²Department of Human Metabolism, School of Medicine, University of

Sheffield, Sheffield, UK. ¹³Department of Dermatology, Royal Hallamshire Hospital, Sheffield, UK. ¹⁴Department of Pathophysiology and ¹⁵Department of Dermatology, University of Tartu and Department of Dermatology, Tartu University Hospital, Tartu, Estonia. ¹⁶Department of Molecular Genetics & Microbiology, and ¹⁷Department of Pathology, Immunology, and Laboratory Medicine, University of Florida College of Medicine, Gainesville, Florida, USA. ¹⁸Lumiderm, Madrid, Spain. ¹⁹Section of Dermatology, Department of Surgery and Translational Medicine, University of Florence, Italy and Ospedale Piero Palagi, Florence, Italy. ²⁰Laboratorio Fisiopatologia Cutanea, Istituto Dermatologico San Gallicano, Rome, Italy. ²¹Department of Dermatology, Columbia University College of Physicians and Surgeons, New York, New York, USA and ²²Pediatric and Adolescent Dermatology, St. Luke's-Roosevelt Hospital Center, New York, New York, USA. ²³International Vitiligo Center, Uppsala, Sweden. ²⁴Vitiligo Research Foundation, New York, New York, USA. ²⁵Institute of Gene Biology, Russian Academy of Sciences, Moscow, Russia. ²⁶Department of Dermatology, University of Münster, Münster, Germany. ²⁷Department of Dermatology, Henry Ford Health System, Detroit, Michigan, USA.

Correspondence should be addressed to R.A.S. (richard.spritz@ucdenver.edu).

Vitiligo is an autoimmune disease in which depigmented skin results from destruction of skin melanocytes, with strong epidemiologic association with several other autoimmune diseases. In previous linkage and genome-wide association studies (GWAS1, GWAS2), we identified 27 vitiligo susceptibility loci in patients of European (EUR) ancestry. We carried out a third GWAS (GWAS3) of vitiligo in EUR subjects, with augmentation of GWAS1 and GWAS2 controls, genome-wide imputation, and meta-analysis of all three vitiligo GWAS, followed by an independent replication study. The combined analyses, with 4,680 vitiligo cases and 39,586 controls, identified 23 novel replicated loci, as well as 7 new suggestive loci, most encoding immune regulators, apoptotic regulators, and melanocyte regulators, several of which are also associated with other autoimmune diseases. Functional analyses indicate a predominance of causal regulatory variation, in some cases corresponding to eQTL at these loci. Together, the identified genes provide a framework for vitiligo genetic architecture and pathobiology, highlight genetic relationships to other autoimmune diseases and melanoma, and offer potential targets for vitiligo treatment.

Vitiligo is a complex autoimmune disease characterized by white patches of skin due to destruction of melanocytes in involved regions¹. Vitiligo is epidemiologically associated with several other autoimmune diseases, both in vitiligo patients and their close relatives². In previous genomewide linkage and association studies we identified 27 vitiligo susceptibility loci³⁻⁶ in EUR subjects, principally encoding immunoregulatory proteins, many of which are also associated with other autoimmune diseases⁷. Several other vitiligo genes encode melanocyte components that regulate normal pigmentary variation⁸ and in some cases are major vitiligo autoimmune antigens, with an inverse association of variation at these loci with vitiligo versus malignant melanoma^{4,6}.

To detect additional vitiligo loci with lower odds ratios (ORs), as well as uncommon risk alleles with higher ORs, we carried out a third GWAS (GWAS3) of EUR subjects. We additionally augmented the number of population controls in our previous GWAS1 and GWAS2 and performed genome-wide imputation of all three EUR vitiligo GWAS. After quality control procedures, the augmented GWAS1 included 1,381 cases and 14,518 controls, GWAS2 included 413 cases and 5,209 controls, and GWAS3 included 1,059 cases and 17,678 controls, with genomic inflation factors 1.068, 1.059, and 1.013, respectively. We then carried out a fixed-effects meta-analysis of the three GWAS datasets for 8,966,411 shared markers (Online Methods). Replication was undertaken using an additional 1,827 EUR vitiligo cases and 2,181 controls.

Twenty-three new loci achieved genome-wide significance ($P < 5 \times 10^{-8}$) for association with vitiligo and demonstrated subsequent replication (**Table 1; Supplementary Fig. 1**); 21 are completely novel (FASLG, PTPRC, PPP4R3B, BCL2L11, FARP2, UBE2E2, NRROS, PPP3CA, IRF4, SERPINB9, CPVL, NEK6, ARID5B, BAD, TTBK2, RAB5C, TNFRSF11A, IRF3-BCL2L12, ASIP, PTPN1, and IL1RAPL1), while two, CTLA4 and TICAM1, were suggestive in our previous studies. One previously significant locus, CLNK, was no longer significant (**Supplementary Table 1**). Another potential new locus, PVT1, exceeded genome-wide significance in the discovery meta-analysis ($P = 7.74 \times 10^{-9}$), but could not be successfully genotyped in the replication study and so remains uncertain. Two other loci, FLI1 and LOC101060498, exceeded genome-wide significance in the discovery meta-analysis ($P = 3.76 \times 10^{-8}$ and $P = 3.60 \times 10^{-11}$, respectively), but did not demonstrate replication. Seven additional novel loci achieved suggestive significance ($P < 10^{-5}$) in the discovery meta-analysis (STAT4, PPARGC1B, c7orf72, PARP12, FADS2, CBFA2T3, and a chr17 locus in the vicinity of AFMID) and gave evidence of replication, but failed to achieve overall genome-wide significance (**Supplementary Table 1**). Genome-wide conditional and joint analysis⁹ provided evidence for multiple independent

association signals at six loci (LPP, MHC class I, MHC class II, TG-SLA, IL2RA, MC1R; **Supplementary Table 2**).

Together, the loci identified by meta-analyses of the three GWAS account for approximately 18% of vitiligo heritability ($h^2 \sim 0.75$) (**Table 1**). The ORs for the 23 new confirmed loci were generally lower than those for loci detected previously⁶, 1.15 to 1.27, excepting CPVL (OR = 1.84), ASIP (OR = 1.64), and IL1RAPL1 (OR = 1.77), for which the associated alleles are uncommon (minor allele frequencies 0.03, 0.07, and 0.01, respectively) and thus were not detected in the previous GWAS due to power limitations.

To screen for functional relationships among the confirmed vitiligo genes, we carried out pathway analysis using g:PROFILER¹⁰, PANTHER¹¹, and STRING¹². PANTHER and gPROFILER identified a significantly enriched network of BioGRID interactions, most significant for the GO categories immune response, immune system process, positive regulation of response to stimulus, positive regulation of biological process, and regulation of response to stimulus. STRING identified a large interaction network (**Fig. 1**), with obvious juxtaposition of proteins involved in immunoregulation, T-cell receptor repertoire, apoptosis, antigen processing and presentation, and melanocyte function.

Considering the 23 newly confirmed vitiligo candidate genes, at least ten (CTLA4, TICAM1, PTPRC, FARP2, UBE2E2, NRROS, CPVL, ARID5B, PTPN1, TNFRSF11A, and perhaps also IL1RAPL1) play roles in immune regulation. Six (FASLG, BCL2L11, BCL2L12, SERPINB9, NEK6, BAD) are regulators of apoptosis, particularly involving immune cells. ASIP encodes a regulator of melanocyte gene expression, and IRF4 encodes a transcription factor for both immune cells and melanocytes. Four (PPP3CA, PPP4R3B, TTBK2, RAB5C) have functions that are not obviously relevant to vitiligo or autoimmunity, though PPP3CA may regulate FOXP3 via NFATC2 and is associated with canine lupus¹³.

Strikingly, several vitiligo genes encode proteins that interact physically and functionally. BCL2L11 and BAD are binding partners that promote apoptosis¹⁴. CTLA4 is liganded by CD80

to inhibit T cell activation¹⁵. BCL2L12 binds to and neutralizes caspase 7 (CASP7)¹⁶. SERPINB9 binds to and specifically inhibits granzyme B (GZMB)¹⁷. Eos (IKZF4) binds and is an obligatory co-repressor of FOXP3 in regulatory T cells¹⁸. Agouti signaling protein (ASIP) binds to the melanocortin-1 receptor (MC1R) to down-regulate production of brown-black eumelanin¹⁹. IRF4 cooperates with MITF to activate transcription of TYR²⁰. And the vitiligo-associated HLA-A*02:01:01:01 subtype presents peptide antigens derived from several different melanocyte proteins, including tyrosinase (TYR), OCA2, and MC1R^{4,6,21}. Together, these functional relationships among the identified vitiligo genes appear to highlight key pathways of vitiligo pathogenesis that are beginning to coalesce.

An unexpected finding from vitiligo GWAS has been an inverse genetic relationship between vitiligo and malignant melanoma risk for genes that encode melanocyte structural and regulatory proteins. TYR, OCA2, and MC1R, encode functional components of the melanocyte and are key vitiligo autoantigens. IRF4 encodes a transcription factor for melanocytes as well as lymphoid, myeloid, and dendritic cells²², controlled by alternative tissue-specific enhancers²³. ASIP and PPARGC1B encode paracrine regulators of melanocyte gene expression. All six of these loci play important roles in normal pigimentary variation^{8,24}, and for all six the specific SNPs that are associated with vitiligo risk are also associated with melanoma protection, and vice-versa^{25,26}. The inverse genetic relationship of susceptibility to vitiligo versus melanoma suggests that that vitiligo may represent dysregulated immune surveillance against melanoma^{27,28}, consistent with the threefold reduction in melanoma incidence among vitiligo patients^{29,30}.

Vitiligo is epidemiologically associated with several other autoimmune diseases, including autoimmune thyroid disease, pernicious anemia, rheumatoid arthritis, adult-onset type 1 diabetes, Addison's disease, and lupus^{31,32}. We searched the NHGRI-EBI GWAS Catalog (<http://www.ebi.ac.uk/gwas/>) and PubMed for the 48 genome-wide significant and 7 suggestive vitiligo susceptibility loci for associations with other autoimmune, inflammatory, and immune-

related disorders. As shown in **Fig. 2**, of the 23 novel genome-wide significant vitiligo loci, FASLG has been associated with celiac disease³³ and Crohn's disease³⁴; PTPRC with ulcerative colitis³⁵; BCL2L11 with primary sclerosing cholangitis³⁶; CTLA4 with alopecia areata³⁷, rheumatoid arthritis³⁸, autoimmune thyroid disease^{39,40}, and type 1 diabetes autoantibody production⁴¹; and ARID5B with systemic lupus erythematosus⁴². Of the seven suggestive loci, STAT4 has been associated with Behçet's disease⁴³, Sjögren's syndrome⁴⁴, and lupus⁴⁵; and c7orf72 with lupus⁴⁶. These concordant associations for vitiligo and other autoimmune and inflammatory diseases add to those involving previously identified vitiligo susceptibility loci, which include RERE, PTPN22, IFIH1, CD80, LPP, BACH2, CCR6, SLA, IL2RA, CD44, a chr11q gene desert, IKZF4, SH2B3, UBASH3A, and C1QTNF6^{4,6}.

A majority of loci associated with complex traits involve causal variants that are regulatory in nature⁴⁷⁻⁵¹, often corresponding to apparent expression quantitative trait loci (eQTLs)⁵¹. For TYR²¹, GZMB⁵², and MC1R⁷, principal vitiligo risk derives from missense substitutions, whereas for OCA2⁶ and the MHC class I⁵³ and class II⁵⁴ loci principal vitiligo risk is associated with causal variation in nearby transcriptional regulatory elements. Overall, at 52% of vitiligo loci, the most significant SNPs are within or near a transcriptional regulatory element predicted by ENCODE data^{55,56}. At 16% of loci, the most significant SNPs are within an intron, another 16% are in intergenic regions without known regulatory significance, and only 16% are in coding regions, several resulting in missense substitutions. To assess the general functional categories of apparent causal variants for vitiligo, we applied the stratified LD score regression method⁵⁰ to the GWAS meta-analysis summary statistics. As shown in **Fig. 3**, greatest enrichment of heritability was observed for markers in regulatory functional categories, with considerably less enrichment of markers in protein coding regions.

We utilized two approaches to assess correspondence of vitiligo association signals with expression of genes in the vicinity. We used PrediXcan⁵⁷ to predict expression of 11,553 genes in whole blood for each study subject, and then test association of expression of each gene with

vitiligo affection status. We used a Bayesian method to assess co-localization of cis eQTL signals in purified blood monocytes with the confirmed vitiligo association signals. The PrediXcan analysis found 83 genes with significant differential expression in vitiligo cases versus controls after Bonferroni correction (**Supplementary Table 3**); of these, 75 were located within 1 Mb of a confirmed vitiligo susceptibility locus, demonstrating highly significant enrichment compared to non-significant PrediXcan results ($P < 0.00001$). The eQTL analysis found that 10 of the confirmed vitiligo association signals showed significant or suggestive co-localization with eQTL identified in purified monocytes (**Supplementary Table 4**). Of the confirmed vitiligo genes that could be tested using both methods, 6 were significant in both analyses (CASP7, HERC2-OCA2, TEF, TICAM1, RERE, RNASET2). For all of these except CASP7, the lead SNP was located within or very close to an ENCODE element likely to regulate gene expression.

Like a jigsaw puzzle, the pieces of the vitiligo pathogenome are thus beginning to fit together, revealing a complex network of immunoregulatory proteins, apoptotic regulators, and melanocyte components that mediate both autoimmune targeting of melanocytes in vitiligo and susceptibility to melanoma. For vitiligo as for other complex diseases, there is enrichment of causal variation in regions that regulate gene expression. This may bode well for identifying potential therapeutic targets, as pharmacologic modulation of dysregulated biological pathways may prove more tractable than attempting to target proteins impacted by amino acid substitutions.

URLs. 1000 Genomes Project, <http://www.1000genomes.org/>; 1000 Genomes Project data, <http://www.sph.umich.edu/csg/abecasis/MACH/download/1000G-2010-08.html>; NHGRI-EBI GWAS Catalog, <http://www.ebi.ac.uk/gwas/>; NIH Database of Genotypes and Phenotypes (dbGaP), <http://www.ncbi.nlm.nih.gov/gap>; Online Mendelian Inheritance in Man (OMIM),

<http://www.ncbi.nlm.nih.gov/omim>; PLINK, <http://pngu.mgh.harvard.edu/purcell/plink/>; STATA, <http://www.stata.com>; STRING database, <http://string-db.org>

ACKNOWLEDGMENTS

We thank the thousands of vitiligo patients and normal control individuals around the world who participated in this study. We thank the Center for Inherited Disease Research (CIDR) for genotyping. This work utilized the Janus supercomputer, which is supported by the National Science Foundation (award number CNS-0821794), the University of Colorado Boulder, the University of Colorado Denver, and the National Center for Atmospheric Research. The Janus supercomputer is operated by the University of Colorado Boulder. This work was supported by grants R01AR045584, R01AR056292, and P30AR057212 from the U.S. National Institutes of Health.

AUTHOR CONTRIBUTIONS

Y.J., G.A. and D.Y. performed statistical analyses. J.S. managed computer databases, software, and genotype data. T.M.F., S.B., G.A., and K.M.B. managed DNA samples and contributed to experimental procedures. P.J.H. managed subject coordination. S.A.B., A.H., A.L., R.M.L., A.W., J.P.W.vdV., N.vG., J.L., D.C.B., A.T., K.E., E.H.K., D.J.G., A.P.W., S.K., E.P., K.K., M.K., .R.W., W.T.M., A.O., S.M., R.C., M.P., N.B.S., M.S., Y.V., I.K., M.B., H.L., I.H., L.Z., and Q.-S.M. provided subject samples and phenotype information. S.A.S., P.R.F. and R.A.S. conceived, oversaw, and managed all aspects of the study. R.A.S. wrote the first draft of the manuscript. All authors contributed to the final paper.

COMPETING FINANCIAL INTERESTS

The authors declare no competing financial interests.

1. Picardo, M. & Taïeb, A. (eds.) Vitiligo (Springer, Heidelberg & New York, 2010).
2. Alkhateeb, A. et al. Epidemiology of vitiligo and associated autoimmune diseases in Caucasian probands and their families. *Pigment Cell Res.* **16**, 208–214 (2003).
3. Jin, Y. et al. NALP1 in vitiligo-associated multiple autoimmune disease. *N. Engl. J. Med.* **356**, 1216-1225 (2007).
4. Jin, Y. et al. Variant of TYR and autoimmunity susceptibility loci in generalized vitiligo. *N. Engl. J. Med.* **362**, 1686–1697 (2010).
5. Jin, Y. et al. Common variants in FOXP1 are associated with generalized vitiligo. *Nat. Genet.* **42**, 576-578 (2010).
6. Jin, Y. et al. Genome-wide association study and meta-analysis identifies 13 new melanocyte-specific and immunoregulatory susceptibility loci for generalized vitiligo. *Nat. Genet.* **44**, 676-680 (2012).
7. Ricano-Ponce I & Wijmenga C. Mapping of immune-mediated disease genes. *Annu. Rev. Genomics Hum. Genet.* **14**, 325–353 (2013).
8. Liu F. et al. Genetics of skin color variation in Europeans: genome-wide association studies with functional follow-up. *Hum Genet.* **134**, 823–835 (2015).
9. Yang, J. et al. Conditional and joint multiple-SNP analysis of GWAS summary statistics identifies additional variants influencing complex traits. *Nat. Genet.* **44**, 369-375 (2012).
10. Reimand, J., Arak, T. & Vilo J. g:Profiler—a web server for functional interpretation of gene lists (2011 update). *Nucleic Acids Res.*, **39**, W307-15 (2011).
11. Mi, H., Poudel, S., Muruganujan, A., Casagrande, J.T. & Thomas P.D. PANTHER version 10: expanded protein families and functions, and analysis tools. *Nucleic. Acids. Res.* **44**, D336-342 (2016).
12. Szklarczyk, D. et al. STRING v10: protein-protein interaction networks, integrated over the tree of life. *Nucleic Acids Res.* **43**, D447-D452 (2015).

13. Wilbe, M., et al. Multiple changes of gene expression and function reveal genomic and phenotypic complexity in SLE-like disease. *PLoS Genet.* **11**, e1005248 (2015).
14. Wang, X., Xing, D., Liu, L. & Chen, W.R. BimL directly neutralizes Bcl-xL to promote Bax activation during UV-induced apoptosis. *FEBS Lett.* **583**, 1873-1879 (2009).
15. Linsley, P.S. et al. Human B7-1 (CD80) and B7-2 (CD86) bind with similar avidities but distinct kinetics to CD28 and CTLA-4 receptors. *Immunity.* **1**, 793-801 (1994).
16. Stegh, A.H. et al. Bcl2L12 inhibits post-mitochondrial apoptosis signaling in glioblastoma. *Genes Dev.* **21**, 98-111 (2007).
17. Sun, J. et al. A cytosolic granzyme B inhibitor related to the viral apoptotic regulator cytokine response modifier A is present in cytotoxic lymphocytes. *J. Biol. Chem.* **271**, 27802-27809 (1996).
18. Pan, F. et al. Eos mediates Foxp3-dependent gene silencing in CD4⁺ regulatory T cells. *Science* **325**, 1142-1146 (2009).
19. Ollmann, M.M., Lamoreux, M.L., Wilson, B.D. & Barsh, G.S. Interaction of Agouti protein with the melanocortin 1 receptor in vitro and in vivo. *Genes Dev.* **12**, 316-330 (1998).
20. Praetorius, C. et al. A polymorphism in IRF4 affects human pigmentation through a tyrosinase-dependent MITF/TFAP2A pathway. *Cell* **155**, 1022-1033 (2013).
21. Jin, Y. et al. Next-generation DNA re-sequencing identifies common variants of TYR and HLA-A that modulate the risk of generalized vitiligo via antigen presentation. *J. Invest. Dermatol.* **132**, 1730-1733 (2012).
22. Gualco, G., Weiss, L.M. & Bacchi, C.E. MUM1/IRF4. A review. *Appl. Immunohistochem. Mol. Morphol.* **18**, 301-310 (2010).
23. Visser, M., Palstra, R.J. & Kayser, M. Allele-specific transcriptional regulation of IRF4 in melanocytes is mediated by chromatin looping of the intronic rs12203592 enhancer to the IRF4 promoter. *Hum. Mol. Genet.* **25**, 2629-2661 (2015).

24. Das, P.K., van den Wijngaard R.M.J.G.J., Wankowicz-Kalinska, A. & Le Poole, I.C. A symbiotic concept of autoimmunity and tumour immunity: lessons from vitiligo. *Trends Immunol.* **22**, 130-136 (2001).
25. Spritz, R.A. The genetics of generalized vitiligo: autoimmune pathways and an inverse relationship with malignant melanoma. *Genome Med.* **19**, 2:78 (2010).
26. Teulings, H.E. et al. Decreased risk of melanoma and nonmelanoma skin cancer in patients with vitiligo: a survey among 1307 patients and their partners. *Br. J. Dermatol.* **168**, 162-171 (2013).
27. Paradisi, A. et al. Markedly reduced incidence of melanoma and nonmelanoma skin cancer in a nonconcurrent cohort of 10040 patients with vitiligo. *J. Am. Acad. Dermatol.* **71**, 1110-1116 (2014).
28. Nan H. et al. Genome-wide association study of tanning phenotype in a population of European ancestry. *J. Invest. Dermatol.* **129**, 2250-2257 (2009).
29. Read, J., Wadt, K.A. & Hayward, N.K. Melanoma genetics. *J. Med. Genet.* **53**, 1-14 (2016).
30. Shoag, J. et al. PGC-1 coactivators regulate MITF and the tanning response. *Mol. Cell* **49**, 145-157. (2013).
31. Alkhateeb, A. et al. Epidemiology of vitiligo and associated autoimmune diseases in Caucasian probands and their families. *Pigment Cell Res.* **16**, 208-214 (2003).
32. Laberge, G. et al. Early disease onset and increased risk of other autoimmune diseases in familial generalized vitiligo. *Pigment Cell Res.* **18**, 300-305 (2005).
33. Dubois, P.C. et al. Multiple common variants for celiac disease influencing immune gene expression. *Nat. Genet.* **42**, 295-302 (2010).
34. Franke A. et al. Genome-wide meta-analysis increases to 71 the number of confirmed Crohn's disease susceptibility loci. *Nat. Genet.* **42**, 1118-1125 (2010).
35. Juyal, G. et al. Genome-wide association scan in north Indians reveals three novel HLA-independent risk loci for ulcerative colitis. *Gut* **64**, 571-579 (2015).

36. Melum E. et al. Genome-wide association analysis in primary sclerosing cholangitis identifies two non-HLA susceptibility loci. *Nat. Genet.* **43**, 17-19 (2011).
37. Petukhova, L. et al. Genome-wide association study in alopecia areata implicates both innate and adaptive immunity. *Nature* **466**, 113-117 (2010).
38. Gregersen, P.K. et al. REL, encoding a member of the NF-kappaB family of transcription factors, is a newly defined risk locus for rheumatoid arthritis. *Nat. Genet.* **41**, 820-823 (2009).
39. Chu, X. et al. A genome-wide association study identifies two new risk loci for Graves' disease. *Nat. Genet.* **43**, 897-901 (2011).
40. Eriksson, N. et al. Novel associations for hypothyroidism include known autoimmune risk loci. *PLoS One* **7**, e34442 (2012).
41. Plagnol, V. et al. Genome-wide association analysis of autoantibody positivity in type 1 diabetes cases. *PLoS Genet.* **7**, e1002216 (2011).
42. Yang, W. et al. Meta-analysis followed by replication identifies loci in or near CDKN1B, TET3, CD80, DRAM1, and ARID5B as associated with systemic lupus erythematosus in Asians. *Am. J. Hum. Genet.* **92**, 41-51 (2013).
43. Hou, S. et al. Identification of a susceptibility locus in STAT4 for Behcet's disease in Han Chinese in a genome-wide association study. *Arth. Rheumat.* **64**, 4104-4113 (2012).
44. Li, Y. et al. A genome-wide association study in Han Chinese identifies a susceptibility locus for primary Sjogren's syndrome at 7q11.23. *Nat. Genet.* **45**, 1361-1365 (2013).
45. Lee, Y.H., Bae, S.C., Choi, S.J., Ji, J.D. & Song, G.G. Genome-wide pathway analysis of genome-wide association studies on systemic lupus erythematosus and rheumatoid arthritis. *Molec. Biol. Rep.* **39**, 10627-10635 (2012).
46. Han, J.W. et al. Genome-wide association study in a Chinese Han population identifies nine new susceptibility loci for systemic lupus erythematosus. *Nat. Genet.* **41**, 1234-1237 (2009).

47. Corradin, O. & Schcheri, P.C. Enhancer variants: evaluating functions in common disease. *Genome Med.* **6**, 85 (2014).
48. Gusev, A. et al. Partitioning heritability of regulatory and cell-type-specific variants across 11 common diseases. *Am. J. Hum. Genet.* **95**, 535-552 (2014).
49. Paul, D.S. et al. Functional interpretation of non-coding sequence variation: concepts and challenges. *Bioessays* **36**, 191-199 (2014).
50. Finucane, H.K. et al. Partitioning heritability by functional annotation using genome-wide association summary statistics. *Nat. Genet.* **47**, 1228-1235 (2015).
51. Nicolae, D. et al. Trait-associated SNPs are more likely to be eQTLs: annotation to enhance discovery from GWAS. *PLoS Genet.* **6**, e1000888 (2010).
52. Ferrara, T.M., Jin, Y., Gowan, K., Fain, P.R., & Spritz, R.A. Risk of generalized vitiligo is associated with the common 55R-94A-247H variant haplotype of GZMB (encoding Granzyme B). *J. Investig. Dermatol.* **133**, 1677-1679 (2013).
53. Hayashi, M. et al. Autoimmune vitiligo is associated with gain of function by a transcriptional regulator that elevates expression of HLA-A*02:01 in vivo. *Proc. Natl. Acad. Sci. U.S.A.* **113**, 1357-1362 (2016).
54. Cavalli, G. et al. MHC class II super-enhancer increases surface expression of HLA-DR and HLA-DQ and affects cytokine production in autoimmune vitiligo. *Proc. Natl. Acad. Sci. U.S.A.* **113**, 1363-1368 (2016).
55. Shlyueva, D., Stampfel, G. & Stark, A. Transcriptional enhancers from properties to genome-wide predictions. *Nat. Rev. Genet.* **15**, 272-286 (2014).
56. Kellis, M. et al. Defining functional DNA elements in the human genome. *Proc. Natl. Acad. Sci. U.S.A.* **111**, 6131–6138 (2014).
57. Gamazon, E.R. et al. A gene-based association method for mapping traits using reference transcriptome data. *Nat. Genet.* **47**, 1091-1098 (2015).

Figure 1 Bioinformatic functional interaction network analysis of proteins encoded by all confirmed and suggestive vitiligo candidate genes. Unsupervised functional interaction network analysis was carried out using STRING v10¹⁵, considering each of the corresponding proteins as a node and permitting a small number of second-order interactions. No first- or second-order edges were shared with other nodes by ARID5B, CCR6, CPVL, GPR137, IL1RAPL1, LPP, NEK6, RAB5C, RERE, TEF, TTBK2, and UBE2E2. Green, neighborhood; blue, databases; red, experimental evidence. Note that SMEK2 is an alternative name for PPP4R3B.

Figure 2 Concordant associations for vitiligo and other autoimmune and inflammatory diseases. We searched the NHGRI-EBI GWAS Catalog (<http://www.ebi.ac.uk/gwas/>) and PubMed for associations of the 48 genome-wide significant and 7 suggestive vitiligo susceptibility loci with other autoimmune, inflammatory, and immune-related disorders (blue), and for association with normal human pigmentation variation (red). RA, rheumatoid arthritis; T1D, type 1 diabetes mellitus; AITD, autoimmune thyroid disease; SLE, systemic lupus erythematosus; IBD, inflammatory bowel disease; MS, multiple sclerosis; MG, myasthenia gravis; AI hepatitis, autoimmune hepatitis.

Figure 3 Enrichment estimates for functional annotations. The combined CMH GWAS123 summary statistics were analyzed using the stratified LD score regression method utilizing the full baseline model⁵⁰. Regulatory, yellow; protein coding, blue; intron, green. Annotations are ordered by enrichment magnitude. Error bars represent jackknife standard error around the enrichment. For each category, percentage of the total markers in the category is in parentheses. Dashed line represents ratio of 1 (no enrichment). Asterisks indicate enrichment significant at $P < 0.05$ after Bonferroni correction for the 20 categories tested (the categories conserved, repressed, transcribed, and promoter flanking were removed as insufficiently

specific). CTCF, CCCTC-binding factor; DGF, digital genomic footprint; DHS, DNase hypersensitivity site; TFBS, transcription factor binding site; TSS, transcriptional start site; 5' UTR, 5' untranslated region. H3K4me1, H3K4me3, H3K9ac, and H3K27ac are regulatory chromatin marks⁵⁵.

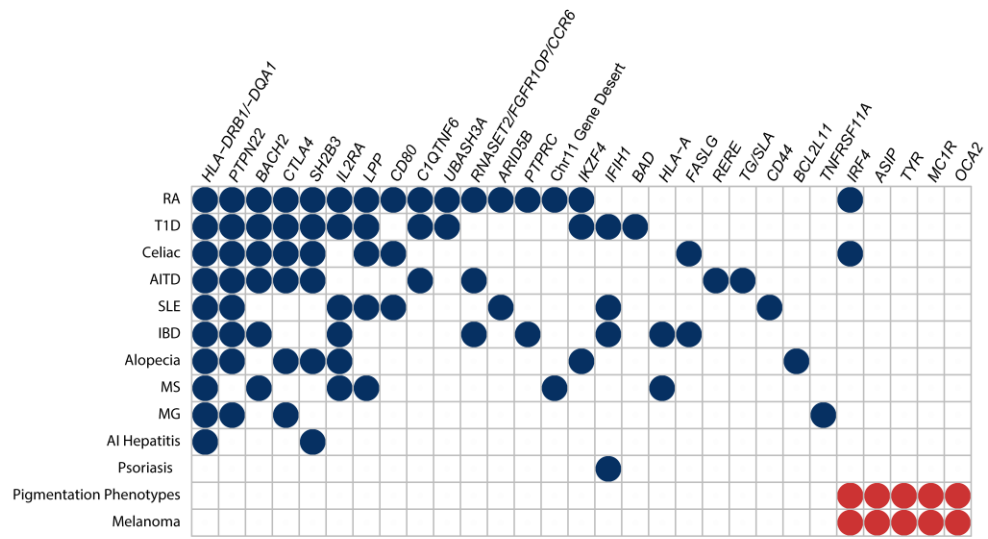
Supplementary Figure 1 Genome-wide meta-analysis results. The genome-wide distribution of $-\log_{10}$ P values from the Cochran-Mantel-Haenszel meta-analysis for 8,966,411 genotyped and imputed markers from GWAS1, GWAS2, and GWAS3 is shown across the chromosomes. The dotted line indicates the threshold for genome-wide significance ($P < 5 \times 10^{-8}$).

Table 1 Allelic associations at vitiligo susceptibility loci following GWAS meta-analysis and replication study

Chr.	Variant	Position (Build 37)	Locus	EA/OA	GWAS123 meta-analysis		GWAS3 replication study		GWAS123 & GWAS3 replication study meta-analysis	
					P value	Odds ratio	P value	Odds ratio	P value	Odds ratio (95% CI)
1	rs301807	8484823	RERE	A/G	1.84 x 10 ⁻¹²	1.22	4.09 x 10 ⁻⁰⁴	1.17	4.14 x 10 ⁻¹⁵	1.21 (1.15-1.27)
1	rs6679677	114303808	PTPN22	A/C	1.60 x 10 ⁻¹⁴	1.39	6.90 x 10 ⁻⁰⁶	1.37	5.43 x 10 ⁻¹⁹	1.39 (1.29-1.49)
1	rs78037977	172715702	FASLG	G/A	1.39 x 10⁻¹³	1.33	8.95 x 10⁻⁰⁵	1.29	6.74 x 10⁻¹⁷	1.32 (1.24-1.41)
1	rs16843742	198672299	PTPRC	C/T	8.84 x 10⁻⁰⁹	0.82	1.87 x 10⁻⁰²	0.88	1.02 x 10⁻⁰⁹	0.83 (0.79-0.88)
2	rs10200159	55845109	PPP4R3B	C/T	3.35 x 10⁻¹³	1.48	3.70 x 10⁻⁰⁷	1.55	3.73 x 10⁻¹⁹	1.51 (1.38-1.66)
2	rs4308124	112010486	BCL2L11	C/T	4.99 x 10⁻⁰⁸	1.17	1.67 x 10⁻⁰²	1.12	3.96 x 10⁻⁰⁹	1.15 (1.10-1.21)
2	rs2111485	163110536	IFIH1	A/G	2.69 x 10 ⁻²²	0.75	8.58 x 10 ⁻⁰⁵	0.83	6.40 x 10 ⁻²⁵	0.77 (0.73-0.81)
2	rs231725	204740675	CTLA4	A/G	2.25 x 10⁻⁰⁸	1.18	1.57 x 10⁻⁰³	1.16	1.49 x 10⁻¹⁰	1.18 (1.12-1.24)
2	rs41342147	242407588	FARP2	A/G	8.03 x 10⁻⁰⁷	0.80	1.25 x 10⁻⁰³	0.80	3.70 x 10⁻⁰⁹	0.80 (0.74-0.86)
3	rs35161626	23512312	UBE2E2	I/D	7.34 x 10⁻⁰⁷	0.87	1.09 x 10⁻⁰²	0.89	3.13 x 10⁻⁰⁸	0.87 (0.83-0.92)
3	rs34346645	71557945	FOXP1	A/C	6.11 x 10 ⁻¹⁴	0.80	4.23 x 10 ⁻⁰⁶	0.81	7.99 x 10 ⁻¹⁹	0.80 (0.76-0.84)
3	rs148136154	119283468	CD80	C/T	5.02 x 10 ⁻¹⁵	1.37	1.74 x 10 ⁻⁰²	1.17	4.58 x 10 ⁻¹⁵	1.31 (1.22-1.40)
3	rs13076312	188089254	LPP	T/C	3.58 x 10 ⁻²²	1.32	3.48 x 10 ⁻¹⁰	1.33	1.61 x 10 ⁻³⁰	1.32 (1.26-1.38)
3	rs6583331	196347253	NRROS	A/T	1.39 x 10⁻⁰⁷	0.86	3.62 x 10⁻⁰²	0.91	2.53 x 10⁻⁰⁸	0.87 (0.83-0.92)
4	rs1031034	102223386	PPP3CA	A/C	4.78 x 10⁻⁰⁶	0.86	2.14 x 10⁻⁰³	0.86	3.43 x 10⁻⁰⁸	0.86 (0.81-0.91)
6	rs12203592	396321	IRF4	T/C	1.03 x 10⁻⁰⁹	0.77	3.17 x 10⁻⁰⁸	0.68	8.86 x 10⁻¹⁶	0.75 (0.70-0.80)
6	rs78521699	2908591	SERPINB9	G/A	3.33 x 10⁻⁰⁶	0.79	2.27 x 10⁻⁰³	0.80	2.54 x 10⁻⁰⁸	0.79 (0.73-0.86)
6	rs60131261	29937335	HLA-A	D/I	2.63 x 10 ⁻⁴⁸	1.53	8.01 x 10 ⁻²⁰	1.54	1.56 x 10 ⁻⁶⁶	1.54 (1.46-1.61)
6	rs9271597	32591291	HLA-DRB1/DQA1	A/T	3.15 x 10 ⁻⁸⁹	1.77	nd	nd	nd	nd
6	rs72928038	90976768	BACH2	A/G	1.12 x 10 ⁻¹¹	1.28	2.04 x 10 ⁻⁰⁴	1.25	1.00 x 10 ⁻¹⁴	1.27 (1.19-1.35)
6	rs2247314	167370230	RNASET2- FGFR1OP-CCR6	C/T	1.97 x 10 ⁻¹³	0.79	1.56 x 10 ⁻⁰⁶	0.79	1.72 x 10 ⁻¹⁸	0.79 (0.75-0.84)
7	rs117744081	29132279	CPVL	G/A	3.74 x 10⁻²²	1.95	1.88 x 10⁻⁰⁶	1.66	8.72 x 10⁻²⁶	1.84 (1.64-2.06)
8	rs2687812	133931055	SLA	A/T	1.98 x 10 ⁻¹¹	1.21	1.69 x 10 ⁻⁰³	1.15	2.19 x 10 ⁻¹³	1.19 (1.14-1.25)
9	rs10986311	127071493	NEK6	C/T	5.45 x 10⁻⁰⁷	1.16	5.10 x 10⁻⁰³	1.14	1.01 x 10⁻⁰⁸	1.15 (1.10-1.21)
10	rs706779	6098824	IL2RA	C/T	1.30 x 10 ⁻²⁴	0.74	9.25 x 10 ⁻⁰⁵	0.84	7.20 x 10 ⁻²⁷	0.77 (0.73-0.81)
10	rs71508903	63779871	ARID5B	T/C	1.09 x 10⁻⁰⁶	1.18	1.52 x 10⁻⁰³	1.19	6.93 x 10⁻⁰⁹	1.18 (1.12-1.25)
10	rs12771452	115488331	CASP7	A/G	9.16 x 10 ⁻⁰⁸	0.83	8.42 x 10 ⁻⁰⁶	0.79	4.43 x 10 ⁻¹²	0.82 (0.78-0.87)

11	rs1043101	35274829	CD44-SLC1A2	G/A	2.08×10^{-13}	1.24	4.20×10^{-06}	1.24	5.26×10^{-18}	1.23 (1.18-1.29)
11	rs12421615	64021605	PLCB3-BAD-GPR137	A/G	3.38×10^{-06}	0.87	3.78×10^{-03}	0.87	4.81×10^{-08}	0.87 (0.83-0.91)
11	rs1126809	89017961	TYR	A/G	7.13×10^{-32}	0.67	2.54×10^{-13}	0.68	1.16×10^{-43}	0.67 (0.63-0.71)
11	rs11021232	95320808	Gene desert	C/T	1.01×10^{-21}	1.38	3.81×10^{-04}	1.22	2.10×10^{-23}	1.34 (1.26-1.41)
12	rs2017445	56407072	IKZF4	A/G	3.81×10^{-20}	1.31	1.22×10^{-12}	1.40	6.62×10^{-31}	1.33 (1.27-1.40)
12	rs10774624	111833788	SH2B3	A/G	1.88×10^{-14}	0.80	1.52×10^{-10}	0.75	6.22×10^{-23}	0.79 (0.75-0.83)
13	rs35860234	43070206	TTBK2	G/T	2.82×10^{-06}	1.16	3.45×10^{-04}	1.20	4.76×10^{-09}	1.17 (1.11-1.23)
14	rs8192917	25102160	GZMB	C/T	1.37×10^{-10}	1.23	1.23×10^{-06}	1.29	8.91×10^{-16}	1.25 (1.18-1.32)
15	rs1635168	28535266	OCA2-HERC2	A/C	6.97×10^{-13}	1.43	7.45×10^{-03}	1.25	8.78×10^{-14}	1.37 (1.26-1.49)
16	rs4268748	90026512	MC1R	C/T	1.63×10^{-20}	0.73	8.23×10^{-15}	0.66	2.88×10^{-33}	0.71 (0.67-0.75)
17	rs11079035	40289012	RAB5C	A/G	3.20×10^{-06}	1.18	3.19×10^{-05}	1.28	6.77×10^{-10}	1.21 (1.14-1.29)
18	rs8083511	60028655	TNFRSF11A	C/A	9.42×10^{-10}	1.24	3.23×10^{-02}	1.13	2.81×10^{-10}	1.21 (1.14-1.28)
19	rs4807000	4831878	TICAM1	A/G	1.58×10^{-09}	1.19	2.11×10^{-06}	1.24	1.94×10^{-14}	1.21 (1.15-1.26)
19	rs2304206	50168871	IRF3-BCL2L12	A/G	6.45×10^{-09}	0.82	4.52×10^{-02}	0.90	2.36×10^{-09}	0.84 (0.80-0.89)
20	rs6059655	32665748	RALY-ASIP	A/G	3.58×10^{-13}	0.63	3.08×10^{-08}	0.57	1.04×10^{-19}	0.61 (0.55-0.68)
20	rs6012953	49123043	PTPN1	G/A	1.18×10^{-07}	1.16	1.74×10^{-02}	1.11	9.47×10^{-09}	1.15 (1.10-1.20)
21	rs12482904	43851828	UBASH3A	A/T	5.74×10^{-29}	1.43	1.16×10^{-03}	1.18	5.84×10^{-29}	1.35 (1.28-1.43)
22	rs229527	37581485	C1QTNF6	A/C	1.40×10^{-24}	1.34	1.15×10^{-07}	1.27	1.14×10^{-30}	1.32 (1.26-1.38)
22	rs9611565	41767486	ZC3H7B-TEF	C/T	1.99×10^{-12}	0.78	3.34×10^{-04}	0.82	3.13×10^{-15}	0.79 (0.75-0.84)
x	rs73456411	29737404	IL1RAPL1	T/G	1.57×10^{-07}	1.72	5.90×10^{-03}	1.62	7.34×10^{-10}	1.77 (1.47-2.13)
x	rs5952553	49392721	CCDC22-FOXP3	C/T	1.81×10^{-08}	0.85	3.48×10^{-02}	0.92	1.05×10^{-09}	0.86 (0.82-0.90)

Figure 2



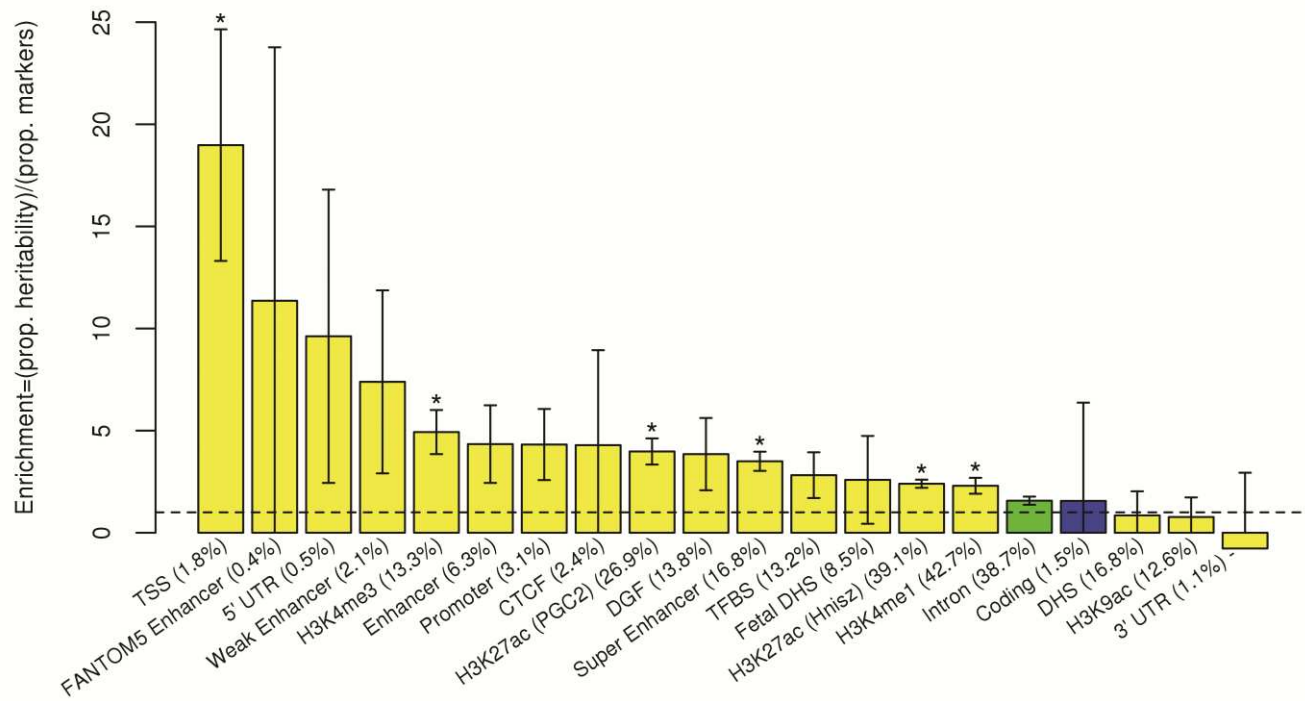


Figure 3